

An improved approach for multiple support response spectral analysis of a long-span high-pier railway bridge

Lanping Li^{1a}, Yizhi bu^{1b}, Hongyu Jia^{*1,2}, Shixiong Zheng^{1c},
Deyi Zhang^{1d} and Kaiming Bi^{3e}

¹Department of Civil Engineering, Southwest Jiaotong University, Chengdu 610031, China

²The Key Laboratory of Urban Security and Disaster Engineering, Beijing University of Technology, Beijing 100124, China

³Center for Infrastructure Monitoring and Protection, School of Civil Engineering and Mechanics, Curtin University, Kent St, Bentley, WA 6102, Australia

(Received June 30, 2016, Revised September 4, 2017, Accepted September 7, 2017)

Abstract. To overcome the difficulty of performing multi-point response spectrum analysis for engineering structures under spatially varying ground motions (SVGM) using the general finite element code such as ANSYS, an approach has been developed by improving the modelling of the input ground motions in the spectral analysis. Based on the stochastic vibration analyses, the cross-power spectral density (c-PSD) matrix is adopted to model the stationary SVGM. The design response spectra are converted into the corresponding PSD model with appropriate coherency functions and apparent wave velocities. Then elements of c-PSD matrix are summarized in the row and the PSD matrix is transformed into the response spectra for a general spectral analysis. A long-span high-pier bridge under multiple support excitations is analyzed using the proposed approach considering the incoherence, wave-passage and site-response effects. The proposed approach is deemed to be an efficient numerical method that can be used for seismic analysis of large engineering structures under SVGM.

Keywords: response spectral analysis; multiple support excitation; stochastic vibration analysis; high-pier railway bridge; seismic spatial variability

1. Introduction

Observations from many previous major earthquakes have clearly revealed that the seismic spatial variability play an important role on the dynamical response of extended structures subjected to seismic ground motion (Kawashima *et al.* 2009, Wang *et al.* 2010). Seismic spatial variability stems mainly from the wave passage effect, coherence effect, and local site effect. In Southwest district of China, the variations of seismic ground motions are more evident due to the complexity of mountainous site topographies. During the recent earthquakes occurred in the mountainous area of China (such as the Wenchuan earthquake of May 12, 2008 and Lushan earthquake of April 20, 2013), it was observed that seismic spatial variability has a significant

effect on the seismic performance of spatially extended structures like the long-span and high-pier railway bridges (Jia *et al.* 2013).

In the dynamical analysis of a long-span high-pier railway bridge, the multiple support excitations may excite the symmetrical mode of vibration largely so that the amplification of structural response can be induced. Extensive studies of ground motion spatial variabilities have been conducted for various types of long-span bridge structures such as suspension bridges (Harichandran *et al.* 1996, Yau *et al.* 2007), cable-stayed bridges (Nazmy *et al.* 1992, Kahan *et al.* 1996, Dumanoglu *et al.* 2003, Soyuluk *et al.* 2004), arch bridges and bridge pounding and isolation (Hao 1997, Hao 1998, Jankowski *et al.* 2000, Zanardo *et al.* 2002, Chou *et al.* 2006, Bi *et al.* 2010, Ates *et al.* 2005), but very few attempts are devoted to the long-span high-pier railway bridges (Jia *et al.* 2013, Zhang *et al.* 2014).

Structural analysis of long-span bridges with spatially varying ground motions (SVGM) is generally performed by time history method or stochastic vibration and response spectrum schemes. Definition of the input time history is a challenging issue for the time history method while the stochastic vibration approach has the drawback of complexity in theory and extensive amount of linear computation (Berrah *et al.* 1992, Kiureghian *et al.* 1981). However, most earthquake resistant design codes in the world specify the response spectrum as the seismic input to obtain the maximum structural responses subjected to seismic waves in terms of the structure design (Cowan *et al.* 2015, Liu *et al.* 2016, Wang *et al.* 2014, Konakli *et al.*

*Corresponding author, Assistant Professor

E-mail: Hongyu1016@swjtu.edu.cn

^aPh.D. Student

E-mail: lilanping@swjtu.edu.cn

^bProfessor

E-mail: yizhibu@163.com

^cProfessor

E-mail: zhengsx@swjtu.edu.cn

^dProfessor

E-mail: zhangdyhit@gmail.com

^eSenior Lecturer

E-mail: kaiming.bi@curtin.edu.au

2011).

Response spectrum analysis has been performed by several attempts for extended structures under multiple support excitations. Two factors on modal spectrum response and modal correlation coefficients are introduced into the usual uniform response spectrum method to account for the wave passage effect and incoherence effect; however, both the local site effect and correlation between static and dynamic terms in structure analysis cannot be modelled (Berrah *et al.* 1992, Berrah *et al.* 1993). The multiple support response spectrum (MSRS) analysis is based on random vibration theory and owns rigorous theoretical basis; however, it needs a large computational effort in structure analysis (Kiureghian *et al.* 1992).

Some simplified methods have been proposed for MSRS analysis, but they are trade-off between accuracy and simplification (Heredia *et al.* 1995). Besides, almost all of the proposed MSRS approaches need a self-developed code that results in the modelling inconvenience for some complex structures such as long-span bridges. On the other hand, the general finite element (FE) software like ANSYS was widely used in structural analysis because of its powerful pre-process, algorithms and post-process procedures. However, those general FE platforms cannot achieve a MSRS analysis for extended structures subjected to SVG. From the practical engineering analysis point of view, it is essential to develop an efficient analysis technique for response spectrum analysis of complex bridge structures.

This paper is devoted to resolve the computational issues of response spectrum method for extended bridge structures under SVG. Section 2 presents a theoretical basis including the improved MSRS theory and implementation of MSRS scheme in the general FE platform ANSYS. Numerical studies are conducted in Section 3 for seismic assessment of a practical high-pier railway bridge under SVG. Conclusions and observations are drawn in Section 4.

2. Theoretical basis

2.1 Modeling of spatially varying ground motions

The cross-power spectral density (c-PSD) function matrix of SVG at m spatial points can be used to model the spatial seismic field as

$$S(i\omega) = \begin{bmatrix} S_{11}(i\omega) & S_{12}(i\omega) & S_{13}(i\omega) & \cdots & S_{1m}(i\omega) \\ S_{21}(i\omega) & S_{22}(i\omega) & S_{23}(i\omega) & \cdots & S_{2m}(i\omega) \\ S_{31}(i\omega) & S_{32}(i\omega) & S_{33}(i\omega) & \cdots & S_{3m}(i\omega) \\ \vdots & \vdots & \vdots & \ddots & \vdots \\ S_{m1}(i\omega) & S_{m2}(i\omega) & S_{m3}(i\omega) & \cdots & S_{mm}(i\omega) \end{bmatrix} \quad (1)$$

In which $S_{mm}(\omega)$ is auto-power spectral density (a-PSD) function at m th excitation point and it can be derived through transformation from response spectra by Eq. (2); $S_{kl}(i\omega) = p_{kl}(i\omega)\sqrt{S_{kk}(i\omega)S_{ll}(i\omega)}$ denotes c-PSD at arbitrary spatial points k and l ;

$p_{kl}(i\omega) = |p_{kl}(i\omega)|\exp(-i\omega d_{kl}^L/v_{app})$ is the coherency function representing the variability of ground acceleration at ground support k and l ; $|p_{kl}(i\omega)|$ denotes the module of coherency function $p_{kl}(i\omega)$; d_{kl}^L is the distance between spatial supports k and l along the wave propagation direction, v_{app} is the apparent wave velocity of seismic motion and $\exp(-i\omega d_{kl}^L/v_{app})$ is the phase part of $p_{kl}(i\omega)$ that represents the wave-passage effect.

The a-PSD (i.e., $S_{mm}(\omega)$) model can be derived from a design response spectrum based on the direct relationship between the PSD function and response spectrum as (Kaul *et al.* 1978)

$$S(i\omega) = \frac{2\xi}{\pi\omega} R^2(\omega) / \left\{ -2\ln \left[\frac{-\pi}{\omega T} \ln(1-r) \right] \right\} \quad (2)$$

In which ξ is a critical damping ratio of 5% in this paper; $R(\omega)$ denotes response spectrum at frequency point ω ; T is the duration of ground motions and is assumed here in to be 25s; r is probability of exceedance of 0.95. The module of coherency function $|p_{kl}(i\omega)|$ proposed by Loh and Yeh (1998) is determined as

$$|p_{kl}(i\omega)| = e^{-a\omega\tau} \cos\omega\tau \quad (3)$$

Where $a=1/(16\pi)$ and τ is the travel time between excitation points k and l .

Based on Eqs. (1) to (3), the PSD matrix for SVG can be constructed and used in Section 2.2 to perform a MSRS analysis for a long-span high-pier railway bridge. The element $S_{kl}(i\omega)$ of c-PSD matrix in Eq.(1) denotes the change of PSD at the k th point due to the seismic excitation at l th point. Namely $S_{kl}(i\omega)$ reveals the nature of these mutual effects on the values of PSD at different ground motion points. Consequently the summation is completed in accordance with the rows of c-PSD matrix. Based on Eq. (1) and the above discussions, the total values of PSD at each excitation point can be expressed by

$$S^P(i\omega) = \sum_{j=1}^m S_{ij} \quad (i=1,2,\dots,m) \quad (4)$$

To carry out the response spectrum analysis of long-span high-pier bridges, Eq. (4) will be transformed to response spectrum values by the inverse function of Eq. (2) as

$$R(\omega) = \sqrt{S^P(i\omega) \left\{ -2\ln \left[\frac{-\pi}{\omega T} \ln(1-r) \right] \right\} \frac{\pi\omega}{2\xi}} \quad (5)$$

Once one can get the total response spectrum values by means of Eq. (5) (in which the spatial variabilities of ground motions have been taken into account), they will be inputted directly into the structure motion equations for MSRS analysis. Moreover, the consideration of spatial variabilities of ground motions is completed before the solution of structural motion equation. Hence the approach proposed in the paper overcomes the difficulty in general

FE software (like ANSYS) that, a complete incoherent analysis of extended structures subjected to SVGGM can be only performed with input spectra uncorrelated to each other. The method proposed herein can be used to carry out dynamical analysis of extended structures subjected to multiple support excitations including the incoherence effect, wave passage effect and local site effect, which is greatly convenient in practical engineering assessment of spatially extended structures under SVGGM using MSRS.

2.2 Method of MSRS analysis

Using the proposed improved modelling approach for seismic inputs in ANSYS, the theoretical derivation of MSRS method is presented in this section for extended lumped mass structures. The coupled equations of motion for a linear discretized, n multi-degree-of-freedom (MDOF), and multiply supported structures under unidimensional translational seismic excitations can be expressed as

$$\begin{bmatrix} M_s & 0 \\ 0 & M_b \end{bmatrix} \begin{bmatrix} \ddot{U}_s \\ \ddot{U}_b \end{bmatrix} + \begin{bmatrix} C_s & C_{sb} \\ C_{bs} & C_b \end{bmatrix} \begin{bmatrix} \dot{U}_s \\ \dot{U}_b \end{bmatrix} + \begin{bmatrix} K_s & K_{sb} \\ K_{bs} & K_b \end{bmatrix} \begin{bmatrix} U_s \\ U_b \end{bmatrix} = \begin{bmatrix} 0 \\ P_b \end{bmatrix} \quad (6)$$

Where the subscripts s and b denote, respectively, the structure and the base; U_s is the n -vector of (total) displacements at the unconstrained DOF; U_b denotes the m -vector of prescribed support displacements; M_s , C_s and K_s are $n \times n$ mass, damping and stiffness matrices, respectively; and P_b is the m -vector of reaction forces at the support DOF. Generally, the total response displacements can be decomposed into the pseudo-static component U_s^s and dynamic one V_s for solving the Eq. (6) as

$$\begin{bmatrix} U_s \\ U_b \end{bmatrix} = \begin{bmatrix} U_s^s \\ U_b \end{bmatrix} + \begin{bmatrix} V_s \\ 0 \end{bmatrix} \quad (7)$$

The pseudo-static component satisfies the following equation without the inertia and damping terms

$$\begin{bmatrix} K_s & K_{sb} \\ K_{bs} & K_b \end{bmatrix} \begin{bmatrix} U_s^s \\ U_b \end{bmatrix} = \begin{bmatrix} 0 \\ P_b^s \end{bmatrix} \quad (8)$$

Due to Eq. (8), we can get U_s^s

$$U_s^s = -K_s^{-1} K_{sb} U_b \quad (9)$$

Substituting Eqs. (7) and (9) into Eq. (6), the dynamic component of the response can be derived in a differential form as

$$M_s \ddot{V}_s + C_s \dot{V}_s + K_s V_s = M_s K_s^{-1} K_{sb} \ddot{U}_b + (C_s K_s^{-1} K_{sb} - C_{sb}) \dot{U}_b \quad (10)$$

Considering the conditions that both stiffness and damping matrices satisfy the rigid body assumption, one can obtain

$$\begin{bmatrix} K_s & K_{sb} \\ K_{bs} & K_b \end{bmatrix} = \begin{bmatrix} E_s \\ E_b \end{bmatrix} + \begin{bmatrix} 0 \\ 0 \end{bmatrix}, \quad \begin{bmatrix} C_s & C_{sb} \\ C_{bs} & C_b \end{bmatrix} = \begin{bmatrix} E_s \\ E_b \end{bmatrix} + \begin{bmatrix} 0 \\ 0 \end{bmatrix} \quad (11)$$

In which E_s and E_b are the rigid displacement vectors

with regard to the active direction of support motion.

From Eq. (11), we can obtain

$$K_{sb} E_b = -K_s E_s, \quad C_{sb} E_b = -C_s E_s \quad (12)$$

For the uniform seismic excitations we have $\ddot{U}_b = E_b \ddot{u}_g$ and can obtain the following Eq. (12)

$$M_s \ddot{V}_s + C_s \dot{V}_s + K_s V_s = -M_s E_s \ddot{u}_g \quad (13)$$

Which is the classical motion equation for a linearly discretized, multi-DOF system under uniform ground motions.

Neglecting the damping term in the forcing function, the motion equation of systems under non-uniform ground motions can be expressed as

$$M_s \ddot{V}_s + K_s V_s = M_s K_s^{-1} K_{sb} \ddot{U}_b \quad (14)$$

This can be commonly solved by modal superposition. Using the transformation $V_s = \Phi Y$ and the orthogonality conditions as well as the assumptions of proportional modes, Eq. (14) can be derived as

$$(\Phi^T M_s \Phi) \ddot{Y} + (\Phi^T C_s \Phi) \dot{Y} + (\Phi^T K_s \Phi) Y = \Phi^T M_s K_s^{-1} K_{sb} \ddot{U}_b \quad (15)$$

The k th modal component can be written as

$$\ddot{y}_k + 2\beta_k \omega_k \dot{y}_k + \omega_k^2 y_k = \gamma_k \ddot{u}_k \quad (16)$$

Where the subscript k denotes the mode number, y_k the modal displacement, β_k the fraction of modal damping, ω_k the modal frequency, and

$$\ddot{u}_k = A_k \ddot{U}_b = \sum_{i=1}^m A_{ki} \ddot{u}_{bi} \quad (17a)$$

$$A_k = \frac{\phi_k^T M_s K_s^{-1} K_{sb}}{\phi_k^T M_s E_s} = [A_{ki}] \quad (17b)$$

$$\gamma_k = \frac{\phi_k^T M_s E_s}{\phi_k^T M_s \phi_k} \quad (17c)$$

Where the index i denotes the degrees of freedom associated with the prescribed support motions; A_k is a row vector with m components A_{ki} and γ_k denotes the k th participation factor.

Based on the stochastic vibration theory, y_k can be calculated by using spectral representation method in solving Eq. (16) and its PSD function can be expressed as

$$S_{y_k}^P = \gamma_k^2 |H_k(\omega)|^2 S_{\ddot{u}_k}(\omega) \quad (18)$$

In which $S_{y_k}^P$ denotes the PSD function of y_k for the case of partially correlated excitations; $H_k(\omega)$ is the k th modal transfer function; and $S_{\ddot{u}_k}(\omega)$ is the PSD function of the modal support motion.

According to Eq. (13), the following equation can be obtained as

$$S_{u_k}(\omega) = \sum_{i=1}^m \sum_{j=1}^m A_{ki} A_{kj} S_{u_{ij}}(\omega) = \left(\sum_{i=1}^m A_{ki}^2 + 2 \sum_{i=1}^{m-1} \sum_{j=i+1}^m A_{ki} A_{kj} \rho_{ij}(\omega, d_{ij}) \right) S_{u_g}(\omega) \quad (19)$$

Where ρ_{ij} denotes the real part of the lagged coherency function representing the incoherence effect of SVGM (also termed as the frequency-dependent spatial correlation coefficient); d_{ij} is the distance between the supports; and $S_{u_g}(\omega)$ is the a-PSD function of ground motion. Eq. (18) can be written in the matrix form as

$$S_{u_k}(\omega) = A_k Q A_k^T S_{u_g}(\omega) \quad (20)$$

In which $Q=[\rho_{ij}]$ denotes the coherency matrix. Based on Eqs. (18) and (20), one obtains

$$S_{yk}^P(\omega) = \gamma_k^2 |H_k(\omega)|^2 A_k Q A_k^T S_{u_g}(\omega) \quad (21)$$

Eq. (21) represents the case of non-uniform excitations; however if the motion is uniform (i.e., $\rho_{ij}=1$), one has

$$S_{yk}(\omega) = \gamma_k^2 |H_k(\omega)|^2 S_{u_g}(\omega) \quad (22)$$

In which S_{yk} is the PSD function of the modal response for fully correlated support excitations. The comparison is conducted in terms of Eqs. (20) and (22), and then it follows that

$$S_{yk}^P(\omega) = A_k Q A_k^T S_{yk}(\omega) \quad (23)$$

As seen from Eq. (23), the relationship between PSD functions for partially correlated support motions and fully correlated motion are developed. Because of a modified method proposed by Berrah and Kausel (1992), one can obtain the relationship between response spectra for the partially correlated support motions and fully correlated motion as

$$R^P(\omega_k, \beta_k) = \sqrt{A_k Q A_k^T} R(\omega_k, \beta_k) \quad (24)$$

In which $R^P(\omega_k, \beta_k)$ is a response spectrum which accounts for the spatial characteristics of ground motions

and $R(\omega_k, \beta_k)$ is a response spectrum for uniform seismic excitations.

As discussed in Section 1.0, all the MSRS method needs to develop a self-code which is impractical for the usage by engineers in the practical engineering application. On the other hand, general FE software like ANSYS (which is acceptable to engineers) can be used an attractive alternative of self-codes for MSRS analysis. However, ANSYS and the other computational FE software can only carry out the analysis of long-span bridges subjected to fully incoherent ground motions. Therefore, this paper presents an improved method in promoting the application of MSRS analysis of practical engineering structures under SVGM. The procedure of the improved approach is presented in details in flow chart of Fig. 1.

It should be noted that the improved MSRS approach is limited to linear elastic analysis by failing to model both the material and geometric nonlinearity; however, the proposed approach can be extended to account for structure nonlinearity using the method like the seismic response modification factor R method.

3. Numerical example of a long-span and high-pier bridge

The proposed scheme in this paper can achieve high computational efficiency, which is particularly attractive in seismic analysis of large and complex practical structures subjected to multiple support ground motions. Hence, a high-pier railway bridge is adopted to demonstrate the practical application of the proposed scheme. For brevity, this section focuses on the local site effect, partially coherent effect and wave passage effect on the longitudinal required separation distance between adjacent bridge segments to avoid multi-sided pounding and the moment at the top and the bottom of high piers. It is noted that effect of the frequency ratio of adjacent bridge segments is ignored for brevity and the dynamical computation in this paper is limited in linear scope.

3.1 Description and model of a high-pier railway bridge

A long-span high-pier continuous rigid frame bridge is employed for the seismic analysis. The railway bridge consists of the left bridge system and the right bridge system and has a total span of 466 m. The left bridge segment is a prestressed-concrete continuous rigid frame system with layout of 81.9 m+168 m+89.05 m, while the right segment is a prestressed-concrete continuous beam system with layout of 33.8 m+56 m+40.1 m. Piers of the railway bridge are numbered from Pier i to Pier m , which have variable hollow cross-sections. These configurations are presented in details in Fig. 2. A 3-D FE model of the high-pier railway bridge selected in the paper is built in a general finite element platform ANSYS. The main girders and piers are modeled by using beam44 element. The combin14 element is used to model the bearings. The mass21 element is adopted to simulate the large masses that

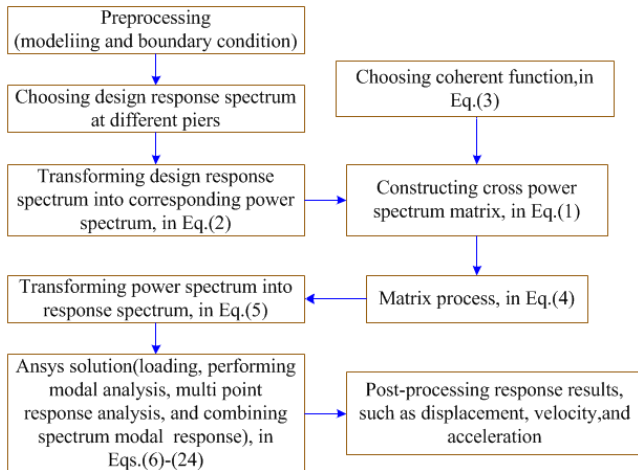


Fig. 1 Flow chart of the improved MSRS approach

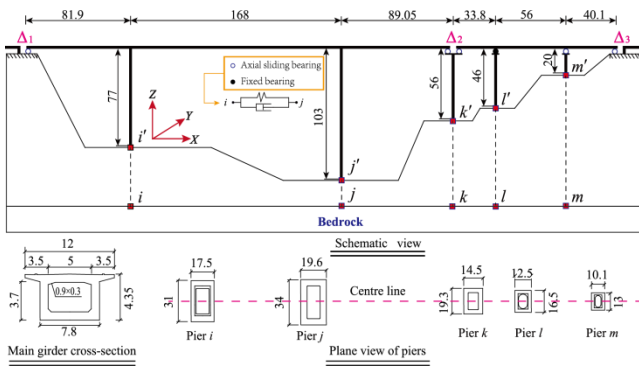


Fig. 2 Schematic view of the railway bridge (unit: m)

Table 1 Material properties

Elements	Materials	Parameters	Values
Bridge girder	C55	Density	2625 (kg/m ³)
		Poisson's ratio	0.2
		Modulus of Elasticity	35.5 (GPa)
		Density	2400 (kg/m ³)
Pier	C45	Poisson's ratio	0.24
		Modulus of Elasticity	32.5 (GPa)

are attached to structural supports in the large mass method. The bottom of Piers *i* to *m* are fixed due to the boundary condition. The vertical DoF(Z), transverse DoF(Y), and the rotational DoF with respect to Z(Rotz) and X(Rotx) directions are fixed both in the north and south abutments of the railway bridge. All DoFs of Pier *i*, Pier *j*, and Pier *l* (the DoF in the connection point of the piers and main girders) are coupled with the corresponding DoF of the main girders, while the longitudinal DoFs(X) in the connection points of pier *k*, pier *m*, and two abutments are connected by the axial sliding bearings with, respectively, different spring stiffness of 47911 (kN/m) in the left abutment, 47878.5 (kN/m) and 16254.5 (kN/m) in pier *k*, 43237 (kN/m) in pier *m*, and 16302.75 (kN/m) in the right abutment. The mechanical properties for the bridge girders and piers are listed in Table 1.

3.2 Analysis case and response spectrum input

3.2.1 Analysis case

To illustrate the implementation of the improved approach proposed in this paper for response spectrum analysis of a long-span high-pier bridge, a total of three cases has been taken into account (Case 1: local site effect+fully incoherence effect; Case 2: local site effect +partially coherence effect; Case 3: local site effect +wave passage effect + coherence effect).

Case 1 can only be performed in ANSYS platform and the other cases cannot be carried out due to the deficiency of FE software. The main objective of this section is to overcome the difficulty that ANSYS can only perform an analysis for local site effect and fully incoherent effect, namely case 1. Moreover, the comparison between different case analysis results is conducted to illustrate the

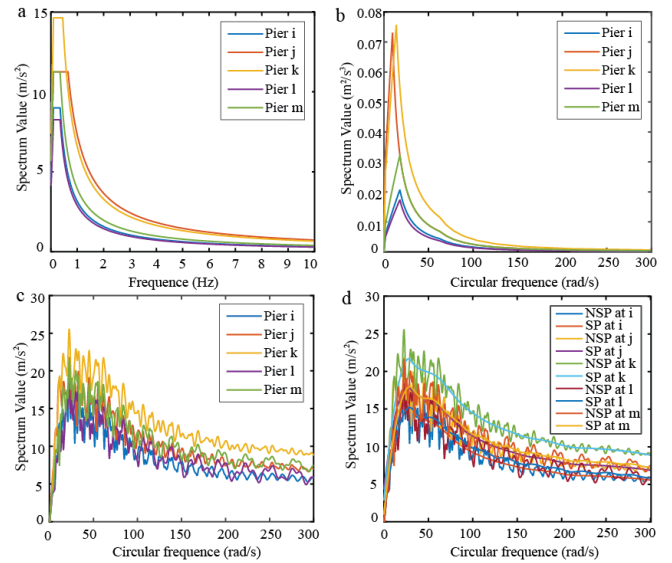


Fig. 3 The seismic input spectra at bottom of pier *i*, *j*, *k*, *l*, and *m*. (a) Design response spectra, (b) Transformed power spectra, (c) Modified response spectra considering ground motion spatial variabilities, (d) Comparison of the smooth and modified response spectra. Note: NSP denotes the spectra curve without smoothing and SP the ones with smoothing.

application of the improved approach in practical seismic analysis of a long-span high-pier bridge subjected to SVGM.

The seismic input spectra at different pier of the long-span high-pier bridge are presented in Fig. 3. The design response spectra for the site conditions under piers *i*, *j*, *k*, *l*, and *m* are given in Fig. 3(a) based on the highway seismic design code of China (2008). The predominant periods for soils under piers *i*, *j*, *k*, *l*, and *m* are 0.35 sec., 0.65 sec., 0.45 sec., 0.35 sec. and 0.35 sec., respectively. The design peak ground acceleration in horizontal direction are 0.2 g, 0.3 g, 0.3 g, 0.2 g, and 0.3 g, respectively. The maximum horizontal design acceleration are 8.99 m/s², 11.24 m/s², 14.61 m/s², 8.24 m/s², and 11.24 m/s², respectively. For taking into account effects of ground motion spatial variation, the design response spectra of Fig. 3(a) is transformed using Eq. (2) into the a-PSD functions shown in Fig. 3(b). The modified response spectra (Case2: L+Partially +Awv300) considering spatial variability of ground motions is presented in Fig. 3(c). As seen from Fig. 3(c), the values of the modified response spectra for SVGM are greater than the ones in Fig. 3(a) without considering spatial variability. For comparisons of the seismic input, the smooth response spectra are adopted and the comparison of smooth response spectra and modified one is given in Fig. 3(d). Finally, the input response spectra used in the MSRS analysis of the employed long-span high-pier bridge can be confirmed according to Fig. 3(d).

3.2.2 Discussion of the input spectra

As observed from Figs. 3(c) and (d), slight fluctuation on the resultant new response spectra curves (i.e., spectra considering the spatial variability effect) at each bottom of

bridge piers is observed. The phenomenon of fluctuation may be due to column superposition from the PSD matrix of Eq. (1) to account for ground motion spatial variability and conversion relation between PSD and response spectra in term of the complex function of Eq. (5).

3.3 Numerical results and discussions

For seismic analysis of the high-pier bridge subjected to SVGM, the circular frequency is bounded between $\omega \in [0\ 300]$ rad/s, the damping ratios of all the modes of interest are assumed to be 0.05. Some seismic responses of interest will be obtained from the numeral analysis, such as the displacements of Nodes 20, 27, 28, 122, 158, 177, 266, and 272, the moments at Node 124, 158 and 268, and the shear forces at Node 124, 158 and 268. The detail nodal layout for structural response of interest is shown in Fig.4. These nodal responses (Node 122, 158, 177, 266, and 272) are mainly for the top and bottom elements of the highest and shortest piers. Other nodes including Nodes 20, 27 and 28 are for elements of the main girder at top of the highest pier and the end elements of the main girder at the connected segment of the two bridge systems.

As seen from Fig. 5(a), the partially coherence effect of ground motion has an important influence on the seismic response of the railway bridge under Case2 (L+ Partially +Aww300). The fully incoherence effect, which only can be performed in ANSYS, has the smallest influence on the seismic response at the same nodes. Consequently it will underestimate the structural response of some key points governing the structural design, if one only uses the module of multiple point response spectrum provided in ANSYS. As seen in Fig. 5(b), the displacement response of beam elements increases first and then decreases with changes of seismic wave velocity from 50(m/s) to 1000(m/s). The

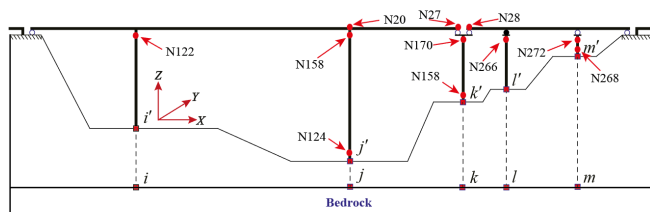


Fig. 4 Node layout of structural response of interest (N20 denotes Node 20 and others are the same means)

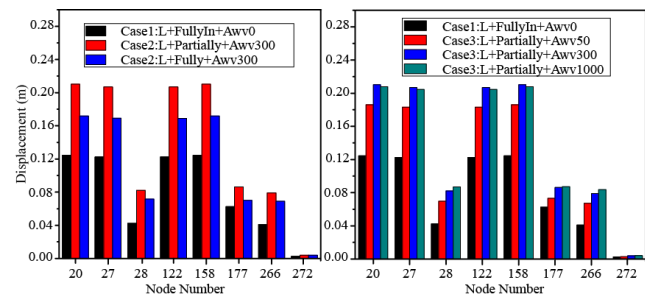


Fig. 5 Node displacement response at key positions of the bridge under Case1, Case2 and Case3. Note: L is expressed as local site condition, Fullyin denotes fully incoherent effect, and Aww stands for apparent wave velocity

Table 2 Nodal displacement of structural response (Unit: m)

Node	Case1	Case2	Case3
20	0.1244	0.2102	0.1718
27	0.1224	0.2069	0.1690
28	0.0425	0.0822	0.0716
122	0.1224	0.2068	0.1690
158	0.1244	0.2102	0.1862
177	0.0625	0.0863	0.0700
266	0.0409	0.0791	0.0671
272	0.0025	0.0038	0.0029

Table 3 Structural moment response (Unit: N·m)

Node	Case1	Case2	Case3
124	4.12E+09	6.78E+09	5.57E+09
158	1.38E+09	2.27E+09	2.61E+09
268	2.10E+08	3.17E+08	3.13E+08

Table 4 Shearing force of structural response (Unit: N)

Node	Case1	Case2	Case3
124	5.56E+07	7.82E+07	7.77E+07
158	2.89E+07	4.17E+07	3.74E+07
268	7.49E+06	1.12E+07	1.06E+07

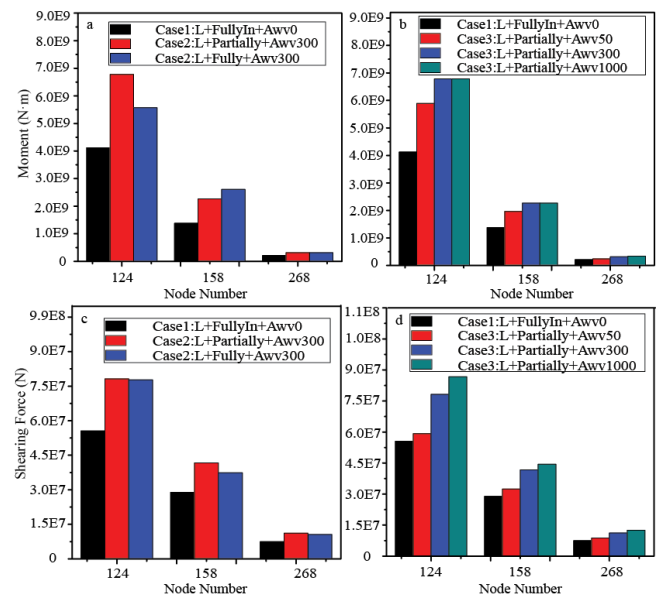


Fig. 6 Nodal internal force of structural response. (a) Moment at Nodes 124, 158, and 268 under Case1 and Case2, (b) Moment at Nodes 124, 158, and 268 under Case1 and Case3, (c) Shear force at Nodes 124, 158, and 268 under Case1 and Case2, (d) Moment at Node 124, 158, and 268 under Case1 and Case3

multiple support excitation phase results in different response results, due to the variation of apparent wave velocity which is a function of frequency of ground motion. The structural response is above 1.5 times under Case1 as large as that of Case3 based on Table 2.

Fig. 6 shows the comparison of internal force of the railway bridge structure under different cases. The nodes such as Node 124, 158 and 268 from the top and bottom of piers are key points for structural design, due to the characteristic of high-pier railway bridges that flexural failure may occur at the highest pier and shear failure at the shortest one. As shown in Fig. 6, the internal force response at Node 124 is the maximum among these selected nodes of interest. At the same time, the combined case with local site effect, partially coherent effect, and passage wave effect with apparent wave velocity 300 (m/s) has the most significant influence on the seismic response and design of the highest pier (the most critical component for the high pier railway bridge). The detailed resultant data are listed in Table 3 and Table 4. Hence it is of prime importance that the improved approach proposed in this paper can achieve the response spectrum analysis of the high-pier railway bridge subjected to SVGM.

4. Conclusions

This paper proposed an improved approach for MSRS analysis of a typical high-pier railway bridge subjected to SVGM considering local site effect, coherence effect, and wave passage effect. The improved approach was based on the general FE platform ANSYS and has widely extended the spectral analysis module of ANSYS to more attractive practical engineering application. A comprehensive and systematic response spectrum analysis approach is derived for spatially extended structures under SVGM. The conclusions are drawn as follow.

- It is inadequate to perform the seismic analysis only through the multi-point response spectrum analysis module of ANSYS, because this may under-estimate the seismic response of structures.
- The proposed modified MSRS method overcomes the difficulty that response spectral analysis of long-span bridges under SVGM is performed inconveniently in general FE platform.
- The modified MSRS method can be readily used in the practical engineering to achieve more accurate and comprehensive seismic analysis of long-span structures.
- Spatial variabilities of ground motions including local site effect, coherent effect, and wave passage effect have important effect on the dynamical seismic response of long-span high-pier bridges, to which the engineers should pay more attention on seismic design of the highest pier.

Acknowledgments

The research for this paper was supported by the National Science Foundation of China (No.51308465) and Postdoctoral Science Foundation of China (No.2015M580031). The authors would like to express their deep gratitude to all the sponsors for the financial aid.

References

- Ates, S., Dumanoglu, A.A. and Bayraktar, A. (2005), "Stochastic response of seismically isolated highway bridges with friction pendulum systems to spatially varying earthquake ground motions", *Eng. Struct.*, **27**(13), 1843-1858.
- Berrah, M. and Kausel, E. (1992), "Response spectrum analysis of structures subjected to spatially varying motions", *Earthq. Eng. Struct. D.*, **21**(6), 461-470.
- Berrah, M.K. and Kausel, E. (1993), "A model combination rule for spatially varying seismic motions", *Earthq. Eng. Struct. D.*, **22**(9), 791-800.
- Bi, K.M., Hao, H. and Chouw, N. (2010), "Required separation distance between decks and at abutments of a bridge crossing a canyon site to avoid seismic pounding", *Earthq. Eng. Struct. D.*, **39**(3), 303-323.
- Chouw, N., Hao, H. and Su, H. (2006), "Multi-sided pounding response of bridge structures with non-linear bearings to spatially varying ground excitation", *Adv. Struct. Eng.*, **9**(1), 55-66.
- Cowan, D.R., Consolazio, G.R. and Davidson, M.T. (2015), "Response-spectrum analysis for barge impacts on bridge structures", *J. Bridge Eng.*, **20**(12), 04015017(1)-04015017(10).
- Dumanoglu, A.A. and Soyluk, K.A. (2003), "Stochastic analysis of long span structures subjected to spatially varying ground motions including the site-response effect", *Eng. Struct.*, **25**(10), 1301-1310.
- Hao, H. (1997), "Stability of simple beam subjected to multiple seismic excitations", *J. Eng. Mech.*, **123**(7), 739-742.
- Hao, H. (1998), "A parametric study of the required seating length for bridge decks during earthquake", *Earthq. Eng. Struct. D.*, **27**(1), 91-103.
- Harichandran, R., Hawwari, A. and Sweidan, B. (1996), "Response of long-span bridges to spatially varying ground motion", *J. Struct. Eng.*, **122**(5), 476-484.
- Heredia, Z.E. and Vanmarcke, E.H. (1995), "Closure on the discussion on seismic random-vibration analysis of multi-support structural systems", *J. Eng. Mech.*, **121**(9), 1037-1038.
- Jankowski, R., Wilde, K. and Fujino, Y. (2000), "Reduction of pounding effects in elevated bridges during earthquakes", *Earthq. Eng. Struct. D.*, **29**(2), 195-212.
- Jia, H.Y., Zhang, D.Y., Zheng, S.X., Xie, W.C. and Pandey, M.D. (2013), "Local site effects on a high-pier railway bridge under tridirectional spatial excitations: Nonstationary stochastic analysis", *Soil Dyn. Earthq. Eng.*, **52**, 55-69.
- Kahan, M. and Gibert, R.J. (1996), "Influence of seismic waves spatial variability on bridges: A sensitivity analysis", *Earthq. Eng. Struct. D.*, **25**(8), 795-814.
- Kaul, M.K. (1978), "Stochastic characterization of earthquakes through their response spectrum", *Earthq. Eng. Struct. D.*, **6**(5), 497-509.
- Kawashima, K., Takahashi, Y. and Ge, H. (2009), "Reconnaissance report on damage of bridges in 2008 Wenchuan, China, Earthquake", *J. Earthq. Eng.*, **13**(7), 965-996.
- Kiureghian, A.D. (1981), "A response spectrum method for random vibration analysis of MDF systems", *Earthq. Eng. Struct. D.*, **9**(5), 419-435.
- Kiureghian, D.A. and Neuenhofer, A. (1992), "Response spectrum method for multi-support seismic excitations", *Earthq. Eng. Struct. D.*, **21**(8), 713-740.
- Konakli, K. and Kiureghian, A.D. (2011), "Extended MSRS rule for seismic analysis of bridges subjected to differential support motions", *Earthq. Eng. Struct. D.*, **40**(12), 1315-1335.
- Liu, G., Lian, J., Liang, C., Li, G. and Hu, J.J. (2016), "An improved complex multiple-support response spectrum method for the non-classically damped linear system with coupled damping", *Bull. Earthq. Eng.*, **14**(1), 161-184.
- Loh, C.H. and Yeh, Y.T. (1988), "Spatial variation and stochastic modeling of seismic differential ground movement", *Earthq.*

- Eng. Struct. D.*, **16**(4), 583-596.
- Nazmy, A.S. and Abdelghaffar, A.M. (1992), "Effects of ground motion spatial variability on the response of cable-stayed bridge", *Earthq. Eng. Struct. D.*, **21**(1), 1-20.
- Soyluk, K. (2004), "Comparison of random vibration methods for multi-support seismic excitation analysis of long-span bridges", *Eng. Struct.*, **26**(11), 1573-1583.
- Wang, F., Zhou, Y. and Wang, S. (2010), "Investigation and assessment of seismic geologic hazard triggered by the Yushu earthquake using geo-spatial information technology", *Disaster Adv.*, **3**(4), 72-76.
- Wang, Z. and Kiureghian, A.D. (2014), "Multiple-support response spectrum analysis using load-dependent Ritz vectors", *Earthq. Eng. Struct. D.*, **43**(15), 2283-2297.
- Yau, J.D. and Fryba, L. (2007), "Response of suspended beams due to moving loads and vertical seismic ground excitations", *Eng. Struct.*, **29**(12), 3255-3262.
- Zanardo, G., Hao, H. and Modena, C. (2002), "Seismic response of multi-span simply supported bridges to a spatially varying earthquake ground motion", *Earthq. Eng. Struct. D.*, **31**(6), 1325-1345.
- Zhang, D.Y., Jia, H.Y., Zheng, S.X., Xie, W.C. and Pandey, M.D. (2014), "A highly efficient and accurate stochastic seismic analysis approach for structures under tridirectional nonstationary multiple excitations", *Comput. Struct.*, **145**, 23-35.